Formation enthalpies of monovacancies in aluminum and gold under the condition of intense laser irradiation

François Bottin[1,2,*] and Gilles Zérah[1,†]

[1]*Département de Physique Théorique et Appliquée, CEA/DAM Ile-de-France BP 12, 91680 Bruyères-le-Châtel Cedex, France*

[2]*LRC, Centre de Mathématiques et de Leurs Applications, CNRS (UMR 8536), ENS Cachan 61, Avenue du Président Wilson, Cachan Cedex, France*

(Received 6 February 2007; published 23 May 2007)

The formation enthalpy of a monovacancy in gold and aluminum under the condition of intense laser irradiation is evaluated by means of *ab initio* calculations. These simulations are performed using norm-conserving pseudopotentials and by taking advantage of an efficient parallelization scheme. Using constant-pressure simulations and for a set of electronic temperatures ranging from 0.01 to 6.0 eV, fully relaxed geometries are thus obtained. Particular attention has been paid to the size of the supercell. We found that calculations up to 108 atoms are needed in order to obtain well-converged thermodynamic quantities. In this respect, the monovacancy formation enthalpy of gold increases more rapidly than for aluminum at high electronic temperatures, leading to a reduction of the monovacancy concentration. This result confirms the increase of the melting temperature and is in good agreement with *ab initio* linear response calculations previously reported.

DOI: 10.1103/PhysRevB.75.174114 PACS number(s): 61.72.Ji, 71.15.−m, 61.72.Bb, 79.20.Ds

I. INTRODUCTION

Over the past few years, the effect of intense laser irradiation on materials has become a significant field of research with many applications ranging from laser surface treatment[1] (ablation, annealing, deposition, etc.) to the understanding of the interstellar medium structure.[2] On the other hand, interest in the thermal behavior of metals before melting, in particular the time scale of the nonequilibrium states during this first-order transition, has also increased.[3–5]

Simulations of short-pulse laser illumination on gold have shown that the ions stand around their initial lattice position during several picoseconds before melting.[6] This nonequilibrium thermal state is usually described by using the so-called two-temperature model[7,8] (TTM) with an initial electronic temperature corresponding to the energy transferred during the laser irradiation and an ionic temperature initially at room temperature. From a fundamental point of view, the strong modification of the electronic structure by the electronic temperature is found to increase this delay.[9]

When considering material undergoing intense laser irradiation, experimental evidence tends to show that melting occurs into the bulk (in a superheated state "from within") and no more at the crystal surfaces (see Refs. 10 and 11 and references therein). In this case, vacancies are known to play a crucial role since the transition occurs and nucleates around low-coordinated atoms and is mediated by structural defects.[12] This melting is easily understood in the framework of Lindemann's theory[13] in which the lattice instabilities are driven by large thermal displacements. In the work of Mukherjee *et al.*, [14] the authors report a correspondence between the monovacancy formation enthalpy of tantalum and melting temperature, which points out the effect of defects on melting. These authors attribute this connection to the similar scaling of the interatomic strength for melting or vacancy creation. This trend occurs over a wide range of pressure (from 0 to 300 GPa), and the same behavior is expected for other metals.

To compute the melting temperature, several attempts were carried out. On the one hand, the evolution of the phonon spectrum with respect to the electronic temperature is computed using density functional perturbation theory (DFPT).[9] Within the framework of the Debye-Lindemann theory[13] and the harmonic approximation,[15] an indication can be obtained about the variation of the melting temperature. More accurate methods are also available to compute directly the melting temperature. *Ab initio* molecular dynamic calculations can be performed using a two-phase (liquid-solid coexistence with an interface) supercell[16] or by computing the free energy of these two phases separately and carrying out a thermodynamic integration.[17,18]

However, these *ab initio* molecular dynamic calculations are extremely demanding and become out of reach in most cases (species with a larger number of electrons, large electronic temperature, etc.). As a consequence, other computational methods are needed to obtain the melting temperature: classical simulations using pair potential as previously done for tantalum[14] and recently for lead[19] or tight-binding potentials.[12,20] For instance, classical molecular dynamics using modified embedded-atom model (MEAM) potential,[21] fitted on *ab initio* equations of state, was successfully used in a previous work[9] and was found to be in reasonable agreement with DFPT results.

These interatomic potentials are fitted on experimental or *ab initio* equilibrium properties and can also include results obtained with nonzero ionic temperature.[22] However, none of them use thermodynamic quantities obtained for high electronic temperature and are not able to reproduce defect-mediated melting after an intense laser irradiation. In order to describe this effect and to conduct molecular dynamics simulations of melting, we need potentials taking into account the evolution of the vacancy formation enthalpy with respect to the electronic temperature.

As prototypical metals, we consider in this work a free-electron-like metal (aluminum) and a noble metal (gold) and compute the vacancy formation enthalpy as a function of the

 ©2007 The American Physical Society

electronic temperature. In our previous work,[9] we found some dissimilarities in their response to intense laser irradiation and the same behavior is expected to take place here for monovacancy formation. In Sec. II, we present a method to compute the thermodynamic quantities in the framework of supercell total-energy calculations as well as the *ab initio* preliminary results obtained for the bulk. We detail in this section the numerical convergences performed with respect to various quantities. In Sec. III, we present and discuss the results obtained for the formation enthalpies and their evolutions with respect to electronic temperature.

II. COMPUTATIONAL METHOD

A. Monovacancy formation enthalpy

A vacancy is created in a perfect bulk lattice when an atom is removed from its bulk position and replaced in a new bulk lattice site. The energy change between these two configurations is the so-called formation energy. In principle, one has to evaluate the energy difference between an initial configuration with N atoms and zero vacancy and a final one with still N atoms but one vacancy. In practice, we perform calculation on a lattice with $N-1$ atoms and one vacancy.

Depending upon the physical conditions, this calculation can be performed in various ways. In order to reproduce the experimental conditions, we use the (N,p,T) ensemble, with p the pressure of the system and T the ionic temperature. The thermodynamic quantity to consider is the monovacancy formation free enthalpy G_{vac}. As a consequence, changes in the internal energy, atomic relaxation, and cell variation (related to modifications of the electronic structure, atomic forces, and stresses, respectively, and their interplay) contribute to the formation enthalpy in this work.

While finite ionic temperature effects should be introduced, we will compute here the formation enthalpy at zero ionic temperature, H_{vac}. At moderate ionic temperature, this is the dominant term and is consistent with our wish to use these results for constructing MEAM potentials. The effect of the electronic temperature T_e is taken into account through a Fermi-Dirac distribution leading to fractional occupations and change in electronic density. In addition, an electronic entropic term $S(N;T_e)$ is added to the internal part $E(N;T_e)$ of the total energy. The new electronic free energy is

$$F_e(N;T_e) = E(N;T_e) - T_e S(N;T_e). \quad (1)$$

As a function of ionic coordinates, the sum of the electronic free energy F_e and the ion Ewald energy correspond to the ionic potential energy and will be denoted E in the following.

As far as the pressure is concerned, particular attention must be paid. Indeed, even if we use a zero-temperature model for the ions, the modification of the electronic density, due to nonzero electronic temperature and vacancy creation, changes indirectly but significantly the forces and stresses.[9] In practice, in order to perform simulations at constant pressure and compute the formation enthalpy, we use the pressure obtained for the bulk system at the equilibrium volume, for each electronic temperature.

The formation enthalpy of the monovacancy, H_{vac}, at constant pressure p is written as an excess quantity:[23–26]

$$H_{\mathrm{vac}}(N;p) = H(N;1;p) - H(N;0;p), \quad (2)$$

with $H(N;\kappa;p)$ the enthalpy of a supercell with N atoms and κ vacancies at pressure p. In supercell calculations, the defective system with N atoms and one isolated vacancy is impossible to construct starting from N atoms in their bulk state. In order use some computable quantities, we replace N by $N-1$ in the previous equation,

$$H_{\mathrm{vac}}(N-1;p) = H(N-1;1;p) - H(N-1;0;p), \quad (3)$$

and compute the second term of the right-hand-side member by using the enthalpy of the system with N atoms. The formation enthalpy of the monovacancy becomes

$$H_{\mathrm{vac}}(N-1;p) = H(N-1;1;p) - \frac{N-1}{N} H(N;0;p). \quad (4)$$

Let us define $\Omega(N) \equiv \Omega(N;0;p)$ and $\Omega(N-1) \equiv \Omega(N-1;1;p)$ as the volumes of the bulk and defective systems, respectively, with $E(N;0;\Omega(N))$ and $E(N-1;1;\Omega(N-1))$ their associated energies. The previous equation is written

$$H_{\mathrm{vac}}(N-1;p) = E_{\mathrm{vac}}(N-1;p) + p\Omega_{\mathrm{vac}}(N-1;p), \quad (5)$$

with $E_{\mathrm{vac}}(N-1;p)$ the formation energy at constant pressure and $\Omega_{\mathrm{vac}}(N-1;p)$ the so-called formation volume of the monovacancy, such as

$$E_{\mathrm{vac}}(N-1;p) = E(N-1;1;\Omega(N-1)) - \frac{N-1}{N} E(N;0;\Omega(N)),$$

$$\Omega_{\mathrm{vac}}(N-1;p) = \Omega(N-1;1;p) - \frac{N-1}{N} \Omega(N;0;p). \quad (6)$$

Equation (5) will be used to compute the formation enthalpy of the monovacancy in gold and aluminum for various electronic temperatures T_e.

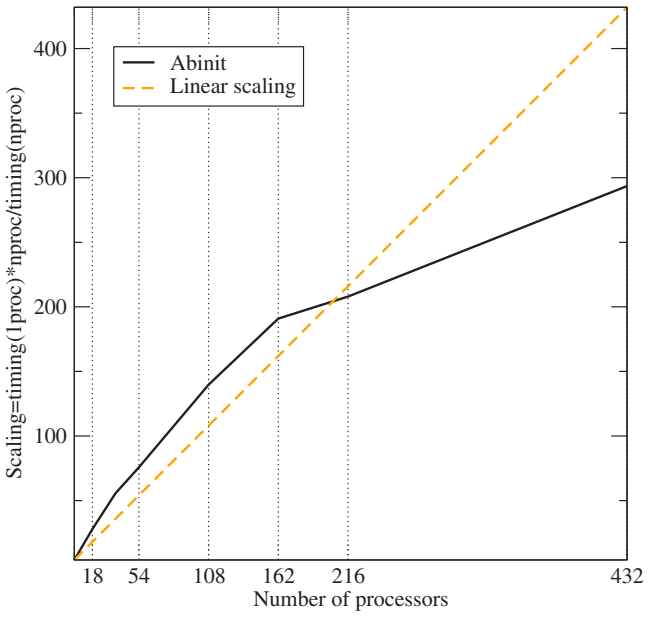

FIG. 1. (Color online) Scaling of the ABINIT code with respect to the number of the processors.

TABLE I. Theoretical and experimental values of the zero-pressure equilibrium volume a_0, bulk modulus B_0, and cohesive energy E_{coh} of gold and aluminum in their fcc phase.

	Gold		Aluminium	
	Present	experiment[a]	Present	experiment[b]
V_0 (Å^3/atom)	17.03	16.96	16.48	16.56
B_0 (GPa)	189.1	173.0	78.4	79
E_{coh} (eV/atom)	4.21		3.45	

[a]Reference 37.
[b]Reference 38.

TABLE II. Number of bands used for gold and aluminum in our calculations for various electronic temperatures and number of atoms (No. atom).

	Gold		Aluminium	
No. atom	31	107	31	107
T_e=0.1 eV	200	650	60	180
T_e=3.0 eV	500	1300	300	900
T_e=6.0 eV	800	1950	600	1980

B. Pseudopotential calculations

Our calculations are performed by using the computational code ABINIT.[27] Norm-conserving pseudopotentials are employed in this study, and a plane-wave basis set is used to expand the wave functions, densities, and potentials. The preconditioned blocked eigenvalue solver LOBPCG[28] in conjunction with an efficient three-dimensional fast Fourier transform[29] (3D-FFT) were implemented. In addition, a double-parallelization scheme over bands and plane waves has been introduced in order to perform these large-scale *ab initio* calculations.[30] Good performances are obtained and a linear scaling is achieved up to 200 processors (see Fig. 1). This efficiency comes from the perfect scaling of the blocked eigenvalue solver and the minimization of the global communications over the two-dimensional processor grid.

In this respect, the monovacancy formation enthalpy is computed for aluminum and gold, a free-electron-like and a noble metal, respectively. Exchange and correlation energy was treated with the local density approximation (LDA) using the Teter-Padé parametrization[31] for gold and with the generalized gradient approximation (GGA) using the Perdew-Burke-Ernzerhof (PBE) parametrization[32] for aluminum. Norm-conserving pseudoptentials are generated following the Troullier-Martins scheme[33] in the Kleinman-Bylander form,[34] considering 12 and 3 electrons as valence for gold and aluminum, respectively. These two pseudopotentials being the ones used in our previous work, the previous and present results can be compared in complete safety, without any ambiguity about exchange and correlation functional or number of electrons.

A cutoff energy equal to 24 and 8 hartrees for gold and aluminum, respectively, is used to reach an accuracy over the total energy lower than 1 mHartree. A careful convergence of the structural parameters with respect to the number of **k** points is performed and a $10\times10\times10$ Monkhorst-Pack (MP) mesh[35] is found to be sufficient for gold, whereas a $14\times14\times14$ is needed for aluminum. These meshes correspond to 110 and 280 k points in the irreducible part of the Brillouin zone (IBZ) when we take into account the symmetry of the fcc cell.

The atomic volume V_0, the bulk modulus B_0, and the cohesive energy E_{coh} of gold and aluminum in their fcc lattice structure are found to be very close to the experimental data (see Table I) and in good agreement with previous *ab initio* calculations (see the work of Bercegeay and Bernard[36] for discussions). We slightly overestimate the atomic volume (0.3%) of gold and underestimate the aluminum one (−0.5%), which are not the common behaviors obtained in the LDA and GGA. These features, although surprising, have been already reported in previous works (see Ref. 36).

C. Numerical convergence

Monovacancy formation enthalpies are computed through supercell calculations. We give in this work the results obtained after optimization of the structural parameters: the atomic positions relax around the vacancy and the lattice parameters change to keep a constant pressure. They are considered to be fully relaxed (well converged) when forces and stresses are lower than 0.5 meV/Å and a 0.03 GPa, respectively.

In order to obtain accurate monovacancy formation enthalpies, a careful convergence with respect to a few parameters has to be carried out. The first one is the number of bands which is chosen to achieve good convergence with respect to the occupation numbers. These numbers of bands

TABLE III. Absolute enthalpy differences (in meV) between various sets of **k** points for each electronic temperature T_e (in eV). The $2\times2\times2$, $4\times4\times4$, $6\times6\times6$, $8\times8\times8$, and $10\times10\times10$ MP meshes lead to 1, 4, 10, 20, and 35 special **k** points in the IBZ, respectively. Results for gold and aluminum are obtained for a 107-atom supercell and separated by the / symbol.

MP meshes	T_e=0.01	T_e=0.1	T_e=0.5	T_e=1.0
$4\times4\times4-2\times2\times2$	55/−179	33/−275	−13/−11	/−6
$6\times6\times6-4\times4\times4$	−5/85	7/96	/3	/
$8\times8\times8-6\times6\times6$	/−84	/−26	/	/
$10\times10\times10-8\times8\times8$	−/12	/	/	/

TABLE IV. Absolute enthalpy differences (in meV) between various sizes of systems (32, 64, and 108 atoms) for three electronic temperatures T_e: 0.1, 3.0, and 6.0 eV. Results for gold and aluminum are separated by the / symbol.

Number of atoms	T_e=0.1	T_e=1.0	T_e=6.0
64-32	−83/90	55/37	3/70
108-64	25/4	−70/1	−182/37

are functions of the number of atoms and electronic temperature T_e and are listed in Table II.

Up to 2000 bands are needed in some calculations, and this number is generally not achievable for standard computational codes. Here, these calculations are feasible thanks to the double parallelization over bands and FFT described in the previous section and in particular the good scalability of our code with respect to the number of bands.

The second parameter to be optimized is the number of **k** points in our supercell calculations used to sample the Brillouin zone. This one, more precisely the IBZ, is known to vary as the inverse of the size of the cell, for a fixed electronic temperature. However, the electronic temperature evolves in these calculations and a convergence with respect to the number of **k** points has to be performed in each case. We show in Table III the absolute differences of the formation enthalpy between various sets of **k** points and for each electronic temperature T_e. The formation enthalpy is exactly computed from Eqs. (6) and (5). For each electronic temperature T_e and set of **k** points we compute the energy of a pseudobulk with 108 atoms and do not multiply by 108 the energy of a fcc cell with one atom. Indeed, in the opposite case, if we would want to achieve a convergence of the enthalpy up to 10 meV, it will be necessary to obtain a convergence lower than 0.1 meV for the fcc cell with one atom, a very demanding accuracy.

In Table III we stop the convergence when the enthalpy differences are around 10 meV. The enthalpy differences fall as a function of the sampling when the electronic temperature increases, and we will neglect these differences for T_e =3.0 or 6.0 eV. As a function of the sampling, these differences decrease more rapidly for gold than for aluminum and calculations up to a $10\times10\times10$ MP mesh are needed in the case of aluminum with a T_e=0.01 eV electronic temperature.

The third parameter to be discussed is the size of the cell: i.e., the number of atoms. Calculations are performed for systems with 32, 64, and 108 atoms (minus one for the systems with one vacancy), and we list again the enthalpy differences in Table IV. If the enthalpy differences are well converged for aluminum, enthalpy differences remain large for gold when T_e increases. A long-range interaction between vacancies, through the periodic conditions, takes place in gold for high electronic temperatures (3.0 and 6.0 eV). This behavior will be discussed thereafter and connected to melting. Calculations up to 216 or 256 atoms are out of reach for T_e=6.0 eV since 2000 bands are already taken into account. Therefore, we will consider the formation enthalpies obtained at T_e=3.0 and 6.0 eV as first steps toward more precise results.

III. RESULTS AND DISCUSSION

We list in Table V the vacancy formation enthalpy of gold and aluminum as a function of the electronic temperature. These ones correspond to a 108-atom supercell size and to the most converged **k**-point mesh. First of all, we will discuss our results at T_e=0 eV and compare them to other works. Since there is no longer a pressure effect for this particular electronic temperature, the enthalpy formation becomes the so-called formation energy. In a second part we will detail our results for higher electronic temperature.

A. Monovacancy formation energy: T_e=0 eV

At exact zero electronic temperature, instabilities in the self-consistent loop, due to degeneracies of the electronic states close to the Fermi level, prevent us from reaching an electronic convergence. We can overcome this drawback by using a broadening of the occupation numbers, the electronic temperature becoming in this case a numerical parameter with no physical meaning. The convergence with respect to electronic temperature (using always a **k**-point-converged mesh) has to be achieved in order to extrapolate a zero-temperature energy. This point is carried out in Table V, and we obtain 0.782 and 0.580 eV for the monovacancy formation energies of gold and aluminum.

In addition, we deduce an error lower than 10 meV. This uncertainty has to be compared with the two uncertainties

TABLE V. Formation enthalpy of a monovacancy, H_{vac}, in gold and aluminum (in eV) for various electronic temperatures T_e. These results are obtained for a 108-atom supercell size. MP meshes are given for each formation enthalpy calculation.

	Gold		Aluminum	
T_e	MP	H_{vac}	MP	H_{vac}
0.01	$6\times6\times6$	0.782	$10\times10\times10$	0.580
0.1	$6\times6\times6$	0.796	$8\times8\times8$	0.591
0.5	$4\times4\times4$	0.804	$6\times6\times6$	0.646
1.0	$2\times2\times2$	0.950	$4\times4\times4$	0.732
3.0	$2\times2\times2$	3.291	$6\times6\times6$	1.517
6.0	$2\times2\times2$	7.327	$6\times6\times6$	2.820

TABLE VI. Formation energy of a monovacancy, H_{vac}, in gold (in eV) at $T_e=0$ eV: present calculation and comparisons with other works. FPLMTO and LSGF-ASA stand for full-potential linear muffin-tin orbitals and locally self-consistent Green's-function method in the atomic-sphere approximation (well suited for close-packed structure), respectively. These two calculations are performed by using a 32-atom cell.

	Present	FPLMTO[a]	LSGF-ASA[b]	Experiment[c]
H_{vac}	0.782	0.71	0.77	0.94

[a]Reference 39.
[b]Reference 26.
[c]Reference 40.

detailed in the previous section (around 10 meV each time at $T_e=0$ eV). These three errors emphasize the weakness of formation energy computed by mean of *ab initio* supercell calculations and the careful convergence needed to obtain reliable quantities. This strong dependence with respect to size, **k**-point mesh, and electronic temperature leads us to add an average error of 40 meV to our formation energy values.

The 0.782 eV value computed for the monovacancy formation energy in gold is in good agreement with other first-principles LDA calculations[26,39] (see Table VI) but underestimate the experimental value.[40] The use of an exchange and correlation functional in its local approximation is generally subject to discussion for cohesive or monovacancy formation energies. However, it yields, to our knowledge, the best result we can expect in the framework of *ab initio* calculations. Indeed, this discrepancy increases when GGA exchange and correlation functionals are employed and a lower value is thus obtained (0.45 eV in Ref. 41). The effects of correlation or relativistic corrections by using LDA+U or spin-orbit coupling, respectively, could ensure a finer description of the electronic properties of this heavy metal and lead to better monovacancy formation energies.

Concerning the formation energy of a monovacancy in aluminum (0.58 eV), its value is also close to other GGA supercell calculations (see values in Table VII). Nonetheless, all previous works obtain the same result: 0.54 eV. As we pointed out, when taking into account the various parameters playing a significant role in this system, this 0.54 eV value corresponds to the lower limit of our 40-meV error bar.

B. Effect of the electronic temperature: $T_e \neq 0$ eV

For both aluminum and gold metals, the monovacancy formation enthalpy increases as a function of the electronic temperature (see Table V). In other words, the energy provided to the system in order to create a monovacancy has to be larger at $T_e=6.0$ eV than at $T_e=0.01$ eV. Whereas this increase of the enthalpy was previously shown by Mukherjee *et al.*[14] for tantalum under pressure, this is highlighted here in the case of gold and aluminum after an ultrafast laser irradiation.

As displayed in the left panel of Fig. 2, this trend of the enthalpy is still connected to an increase of the system pressure. This is not an external pressure, as in the work of Mukherjee *et al.*, but a consequence of the modification of the electronic distribution due to a variation of the electronic temperature. Concerning aluminum, this feature is attributed to the excited electrons which behave as free like when T_e increases. In this case, the increase of the pressure is only related to an increase of its kinetic part (see the left panel of Fig. 3); the other contributions remaining nearly constant.

As far as gold is concerned, a more complicated picture is obtained. At odds with aluminum, the kinetic part of the pressure decreases (see the right panel of Fig. 3). As displayed in Fig. 4, this behavior is due to a slight delocalization of the electronic density when the electronic temperature increases.[48] The behavior of the Hartree and pseudopotential parts are also connected to this variation of the electronic density when T_e increases (see the plane-wave formulation of stress in the work of Nielsen and Martin[47]).

In conclusion, for these two prototypical metals, two different contributions lead to a pressure increasing: for aluminum, the electrons being free like, the process is kinetic, whereas for gold, the orbitals being localized, the process comes from a delocalization of the electronic density. We note that the pressure increase is 2 times larger in gold than in aluminum.

The formation volume $\Omega_{vac}(T_e)$ and formation energy $E_{vac}(T_e)$ of the monovacancy evolve in the same way as the pressure. The ratios $\frac{\Omega_{vac}(T_e)}{\Omega_{vac}(0)}$ and $\frac{E_{vac}(T_e)}{E_{vac}(0)}$ are still approximately 2 times larger in gold than in aluminum. The behavior of these three thermodynamical quantities (pressure, formation energy, and volume of the monovacancy) leads to an increase of the formation enthalpy 2 times faster for gold than for

TABLE VII. Formation energy of a monovacancy H_{vac} in aluminum (in eV) at $T_e=0$ eV: present calculation and comparisons with other works. NC and PAW stand for norm conserving and projector augmented-wave (Ref. 42), respectively. N indicates the number of atoms in the simulation cell, and MP corresponds to the Monkhorst-Pack mesh. In Ref. 43, the **k**-point sampling is not precisely indicated.

	Present	NC[a]	PAW[b]	PAW[c]	Experiment[d]
H_{vac}	0.58±0.04	0.54	0.54	0.54	0.67±0.03
MP	10×10×10	···	16×16×16	4×4×4	
N	108	64	32	108	

[a]Reference 43.
[b]Reference 44.
[c]Reference 45.
[d]Reference 46.

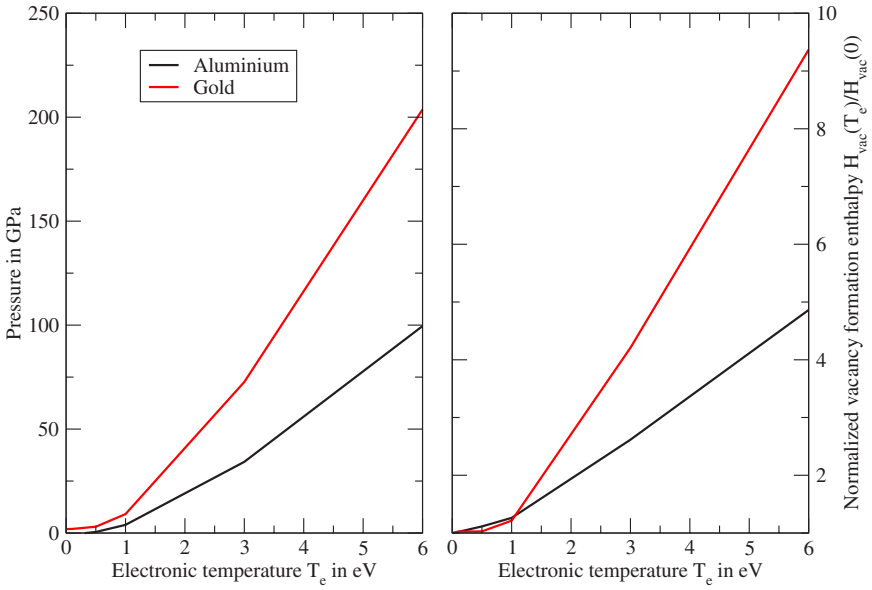

FIG. 2. (Color online) Increase of pressure (left panel) and relative formation enthalpy of a monovacancy $H_{\mathrm{vac}}(T_e)/H_{\mathrm{vac}}(0)$ (right panel) in gold and aluminum as a function of the electronic temperature T_e.

aluminum (see the right panel of Fig. 2). This feature emphazises that monovacancies are more and more difficult to create in gold with respect to aluminum when the electronic temperature increases.

This result about monovacancy creation gives an indication concerning the monovacancy concentration $C_V(T_e)$ achieved in the material. By using the monovacancy formation enthalpy $H_{\mathrm{vac}}(T_e)$ and an Arrhenius' law, the concentration of monovacancy becomes $C_V(T_e,T)=\exp\frac{-H_{\mathrm{vac}}(T_e)}{K_BT}$, with T_e and T the electronic and ionic temperatures. Note that T is lower than the melting temperature in our model since we are interested in the nonequilibrium state before the transition. At a fixed ionic temperature and as a function of the electronic temperature, the formation enthalpies increase (see Table V) and the monovacacy concentrations in gold and aluminum decrease. This fall in the monovacancy concentration is even several orders of magnitude higher in gold than in aluminum. In order to get the same monovacancy concentration at 6.0 eV as at 0 eV, a 5 (10) times larger ionic temperature have to be reached in aluminum (gold).

As far as intense laser irradiation is concerned, we believe that monovacancies play a role which exacerbates the melting process. Indeed, whatever the electronic temperature, they are known to be responsible for melting (when it is initiated in bulk), since the low-coordinated atoms surrounding the defaults undergo large thermal displacements. We find that monovacancy production decreases when the electronic temperature increases. We further point out that this effect is more pronounced in gold than in aluminum. As previously emphasized, in order to keep constant the monovacancy concentration, the melting temperature has to be 5 or 10 times larger. Consequently, we attribute the delay of melting observed in gold after an intense laser illumination to this lack of vacancy in the materials during this nonequilibrium state. This behavior is in good agreement with the large (small) increase of the melting temperature obtained in gold (aluminum) and computed by means of DFPT.[9] Even if,

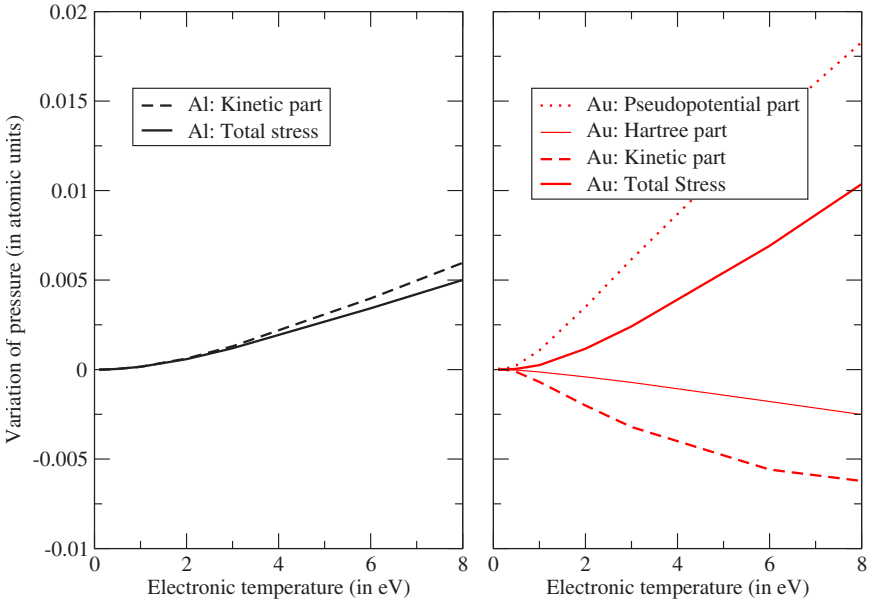

FIG. 3. (Color online) The various parts contributing to the pressure as a function of the electronic temperature. In the left (right) panel we display the results concerning aluminum (gold).

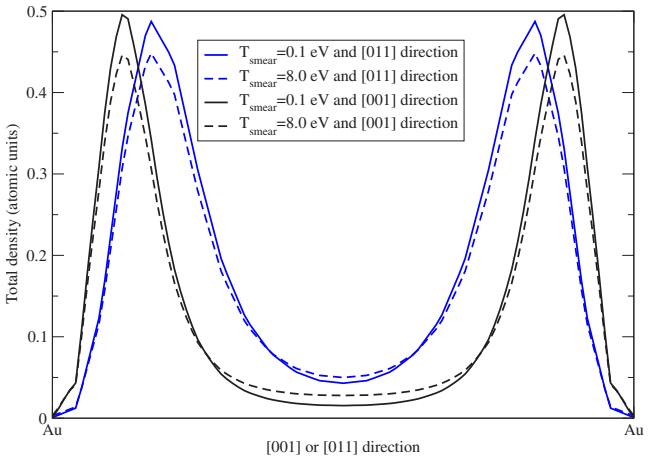

FIG. 4. (Color online) Variation of the electronic density of gold along the [001] and [011] directions as a function of the electronic temperature.

qualitatively, the variations obtained are similar, quantitatively, we overestimate the melting temperature. A more sophisticated model have to be employed in order to get reliable quantities.

IV. CONCLUSION

The formation enthalpies of a monovacancy in gold and aluminum, as a function of the electronic temperature T_e, are computed by means of *ab initio* calculations. We have paid a particular attention to **k**-point sampling, supercell size, and electronic temperature in order get well-converged quantities. Whereas the formation enthalpy of a monovacancy in aluminum increases by a factor 5 between T_e=0.01 eV and T_e=6.0 eV, a factor of 10 is obtained for gold. This higher formation enthalpy confirms that melting becomes more difficult in gold than in aluminum as the electronic temperature increases. These results would allow the construction of interatomic potentials that could be fitted to the electronic temperature-dependent quantities. These potentials are needed to conduct molecular dynamics simulations of melting up to a few thousand atoms.

ACKNOWLEDGMENTS

The calculations have been performed at the Centre de Calcul Recherche et Technologie and at the TERA-10 supercomputer, CEA/DAM Ile-de-France. The authors thank J. Clerouin, F. Lambert, S. Mazevet, and V. Recoules for their help in understanding intense laser irradiation effects, A. Knyazev for fruitful discussions about the LOBPCG blocked eigensolver, and A. Curioni as concerns the double-parallelization technique.

*Electronic address: Francois.Bottin@cea.fr
†Electronic address: Gilles.Zerah@cea.fr

[1] L. Zhang, H. Li, K.-T. Yue, S.-L. Zhang, X. Wu, J. Zi, Z. Shi, and Z. Gu, Phys. Rev. B **65**, 073401 (2002).
[2] D. R. Farley, K. G. Estabrook, S. G. Glendinning, S. H. Glenzer, B. A. Remington, K. Shigemori, J. M. Stone, R. J. Wallace, G. B. Zimmerman, and J. A. Harte, Phys. Rev. Lett. **83**, 1982 (1999).
[3] O. P. Uteza, E. G. Gamaly, A. V. Rode, M. Samoc, and B. Luther-Davies, Phys. Rev. B **70**, 054108 (2004).
[4] K. Widmann, T. Ao, M. E. Foord, D. F. Price, A. D. Ellis, P. T. Springer, and A. Ng, Phys. Rev. Lett. **92**, 125002 (2004).
[5] A. M. Lindenberg, J. Larsson, K. Sokolowski-Tinten, K. J. Gaffney, C. Blome, O. Synnergren, J. Sheppard, C. Caleman, A. G. MacPhee, D. Weinstein *et al.*, Science **308**, 392 (2005).
[6] S. Mazevet, J. Clérouin, V. Recoules, P. M. Anglade, and G. Zérah, Phys. Rev. Lett. **95**, 085002 (2005).
[7] S. I. Anisimov, B. L. Kapeliovich, and T. L. Perel'man, Zh. Eksp. Teor. Fiz. **66**, 776 (1974) [Sov. Phys. JETP **39**, 375 (1975)].
[8] E. Carpene, Phys. Rev. B **74**, 024301 (2006).
[9] V. Recoules, J. Clérouin, G. Zérah, P. M. Anglade, and S. Mazevet, Phys. Rev. Lett. **96**, 055503 (2006).
[10] M. Forsblom and G. Grimvall, Phys. Rev. B **72**, 054107 (2005).
[11] M. Forsblom and G. Grimvall, Nat. Mater. **4**, 388 (2005).
[12] F. Delogu, Phys. Rev. B **73**, 184108 (2006).
[13] F. Lindemann, Phys. Z. **11**, 609 (1910).
[14] S. Mukherjee, R. Cohen, and O. Gülseren, J. Phys.: Condens. Matter **15**, 855 (2003).
[15] C. Lee and X. Gonze, Phys. Rev. B **51**, 8610 (1995).
[16] T. Ogitsu, E. Schwegler, F. Gygi, and G. Galli, Phys. Rev. Lett. **91**, 175502 (2003).
[17] O. Sugino and R. Car, Phys. Rev. Lett. **74**, 1823 (1995).
[18] X. Wang, S. Scandolo, and R. Car, Phys. Rev. Lett. **95**, 185701 (2005).
[19] F. Cricchio, A. B. Belonoshko, L. Burakovsky, D. L. Preston, and R. Ahuja, Phys. Rev. B **73**, 140103(R) (2006).
[20] H. Chamati and N. Papanicolaou, J. Phys.: Condens. Matter **16**, 8399 (2004).
[21] M. I. Baskes, Phys. Rev. Lett. **59**, 2666 (1987).
[22] G. Grochola, S. Russo, and I. Snook, J. Chem. Phys. **123**, 204719 (2005).
[23] A. D. Vita and M. J. Gillan, J. Phys.: Condens. Matter **3**, 6225 (1991).
[24] M. J. Gillan, J. Phys.: Condens. Matter **1**, 689 (1989).
[25] P. Söderlind, L. H. Yang, J. A. Moriarty, and J. M. Wills, Phys. Rev. B **61**, 2579 (2000).
[26] P. A. Korzhavyi, I. A. Abrikosov, B. Johansson, A. V. Ruban, and H. L. Skriver, Phys. Rev. B **59**, 11693 (1999).
[27] The present results have been obtained through the use of the ABINIT code, a common project of the Université Catholique de Louvain, Corning Incorporated, and other contributors (URL http://www.abinit.org).
[28] A. Knyazev, SIAM J. Sci. Comput. (USA) **23**, 517 (2001).
[29] S. Goedecker, M. Boulet, and T. Deutsch, Comput. Phys. Commun. **154**, 105 (2003).
[30] J. Hutter and A. Curioni, Parallel Comput. **31**, 1 (2005).

[31] S. Goedecker, M. Teter, and J. Hutter, Phys. Rev. B **54**, 1703 (1996).
[32] J. P. Perdew, K. Burke, and M. Ernzerhof, Phys. Rev. Lett. **77**, 3865 (1996).
[33] N. Troullier and J. L. Martins, Phys. Rev. B **43**, 1993 (1991).
[34] L. Kleinman and D. M. Bylander, Phys. Rev. Lett. **48**, 1425 (1982).
[35] H. J. Monkhorst and J. D. Pack, Phys. Rev. B **13**, 5188 (1976).
[36] C. Bercegeay and S. Bernard, Phys. Rev. B **72**, 214101 (2005).
[37] R. Wyckoff, *Crystal structures* (Wiley, New York, 1963).
[38] G. Simmons and H. Wang, *Single Crystal Elastic Constants and Calculated Eleastic Properties: A Handbook* (MIT Press, Cambridge, MA, 1971).
[39] Y. N. Gornostyrev, M. I. Katsnelson, N. I. Medvedeva, O. N. Mryasov, A. J. Freeman, and A. V. Trefilov, Phys. Rev. B **62**, 7802 (2000).
[40] R. O. Simmons and R. W. Balluffi, Phys. Rev. **125**, 862 (1962).
[41] C. Zhang and A. Alavi, J. Am. Chem. Soc. **127**, 9808 (2005).
[42] P. E. Blöchl, Phys. Rev. B **50**, 17953 (1994).
[43] K. Carling, G. Wahnström, T. R. Mattsson, A. E. Mattsson, N. Sandberg, and G. Grimvall, Phys. Rev. Lett. **85**, 3862 (2000).
[44] C. Wolverton, V. Ozolins, and M. Asta, Phys. Rev. B **69**, 144109 (2004).
[45] G. Lu and E. Kaxiras, Phys. Rev. Lett. **94**, 155501 (2005).
[46] P. Ehrhart, P. Jung, H. Schultz, and H. Ullmaier, *Atomic Defects in Metal*, Vol. 25 of Landolt-Börnstein, New Series, Group III (Springer-Verlag, Berlin, 1991).
[47] O. H. Nielsen and R. M. Martin, Phys. Rev. B **32**, 3780 (1985).
[48] Qualitatively, when the electronic localization decreases, we can directly show by using Heisenberg's inequality that the electronic kinetic energy increases.